Vol. 39 (2008) *ACTA PHYSICA POLONICA B* No 7

(N)LO SIMULATION OF CHARGINO PRODUCTION AND DECAY*

T. Robens

Institut für Theoretische Physik E, RWTH Aachen, 52056 Aachen, Germany

J. Kalinowski, K. Rolbiecki

Institute of Theoretical Physics, University of Warsaw
Hoża 69, 00-681 Warsaw, Poland

W. Kilian

Fachbereich Physik, University of Siegen
Walter-Flex-Str. 3, 57068 Siegen, Germany

J. Reuter

Physikalisches Institut, University of Freiburg
Hermann-Herder-Str. 3, 79104 Freiburg, Germany

(Received May 8, 2008)

We consider NLO chargino production and decays at the ILC. For this, we present an NLO extension of the Monte Carlo Event Generator WHIZARD including the NLO production. For photonic corrections, we use both a fixed order and a resummation approach. The latter method evades the problem of negative event weights and automatically includes leading higher order corrections. We present results for cross sections and event generation for both methods. As a first step towards a full NLO Monte Carlo, we consider a LO implementation of the chargino production and subsequent leptonic decay and investigate the precision of the sneutrino mass determination by means of lepton energy distributions in chargino decays. The SM and SUSY backgrounds are included in our study using full matrix elements as well as smearing effects from ISR and beamstrahlung. Without using energy distribution fits, the sneutrino mass can be determined with an error in the percent regime.

PACS numbers: 12.15.Lk, 13.66.Hk, 14.80.Ly

* Presented by T. Robens at the Cracow Epiphany Conference on LHC Physics, Cracow, Poland, 4–6 January 2008.

1. Introduction

In many GUT models, the masses of charginos tend to be near the lower edge of the superpartner spectrum, and can be pair-produced at a first-phase ILC with c.m. energy of 500 GeV. The precise measurement of their parameters (masses, mixings, and couplings) is a key for uncovering the fundamental properties of the Minimal Supersymmetric Standard Model (MSSM) [1]. Regarding the experimental precision which is in the percent regime at the ILC, off-shell kinematics for the signal process, and the reducible and irreducible backgrounds [2] need to be included as well as NLO corrections for chargino production. Here we present the inclusion of the latter [3, 4]. For decay modes, we focus on the leptonic decay with electron and muon in the final state. If sneutrinos decay invisibly into the LSP and a neutrino, this channel provides tools to determine sneutrino masses. Such decays, common in many scenarios within the MSSM, preclude threshold scans since sneutrinos cannot be reconstructed directly. The only possibility to access the sneutrino mass in such a case is to select a cascade decay where the precise determination of kinematic distributions gives access to the sneutrino mass. Although this idea has already been exploited [5], a thorough study of how precise the mass determination for the sneutrino in the environment of the ILC can be has as yet not been made. We study the pollution effects of all reducible and irreducible SM and SUSY backgrounds on the visibility of the signal as well as the precision of the sneutrino and the chargino mass measurements. We restrict ourselves to areas in SUSY parameter space where charginos are within reach of a 500 GeV ILC.

2. Chargino production at LO and NLO

Fixed order approach

The total fixed-order NLO cross section is given by

$$\sigma_{\rm tot}(s, m_e^2) \;=\; \sigma_{\rm Born}(s) + \sigma_{v+s}(s, \Delta E_\gamma, m_e^2) + \sigma_{2\to 3}(s, \Delta E_\gamma, m_e^2)\,,$$

where s is the c.m. energy, m_e the electron mass, and ΔE_γ the soft photon energy cut dividing the photon phase space. The "virtual" contribution σ_v is the interference of the one-loop corrections [6] with the Born term. The collinear and infrared singularities are regulated by m_e and the photon mass λ, respectively. The dependence on λ is eliminated by adding the soft real photon contribution $\sigma_{\rm s} = f_{\rm soft}\,\sigma_{\rm Born}(s)$ with a universal soft factor $f_{\rm soft}(\Delta E_\gamma/\lambda)$ [7]. We break the "hard" contribution $\sigma_{2\to 3}(s, \Delta E_\gamma, m_e^2)$, *i.e.* the real-radiation process $e^-e^+ \to \tilde{\chi}_i^- \tilde{\chi}_j^+ \gamma$, into a collinear and a non-collinear part, separated at a photon acollinearity angle $\Delta\theta_\gamma$ relative to the

incoming electron or positron. The collinear part is approximated by convoluting the Born cross section with a structure function $f_{\rm h}(x;\Delta\theta_\gamma,\frac{m_e^2}{s})$ [8]:

$$\sigma_{\rm h,c}(\Delta E_\gamma,\Delta\theta_\gamma,s) \;=\; \int\limits_{\Delta E_\gamma,0}^{E_{\max},\Delta\theta_\gamma} dx_i\, d\Gamma_2\, f_{\rm h}(x_i)|\mathcal{M}_{\rm b}|^2(x_i,s)\,, \qquad (1)$$

where x_i denotes the momentum fraction of the respective incoming beam after photon radiation and $d\Gamma_2$ the two particle final state phase space. The non-collinear part is generated explicitly using exact three particle final state kinematics.

The total fixed order cross section is implemented in the multi-purpose event generator `WHIZARD` [9,10] using a "user-defined" structure function and an effective matrix element

$$|\mathcal{M}_{\rm eff}|^2 \;=\; (1+f_{\rm soft}(\Delta E_\gamma,\,\lambda))\,|\mathcal{M}_{\rm Born}|^2 \;+\; 2\,{\rm Re}(\mathcal{M}_{\rm Born}\,\mathcal{M}^*_{\rm virt}(\lambda))\,,$$

which contains the Born part, the soft-photon factor and the Born 1-loop interference term. In the soft-photon region this approach runs into the problem of negative event weights [11]: for some values of θ_γ, the $2\to 2$ part of the NLO-corrected squared matrix element is positive definite by itself only if ΔE_γ is sufficiently large. To obtain unweighted event samples, an *ad-hoc* approach is to simply drop events with negative weights before proceeding further.

Resummation approach

Negative event weights can be avoided by resumming higher-order initial radiation using an exponentiated structure function $f_{\rm ISR}$ [12,13]. In order to avoid double-counting in the combination of the ISR-resummed LO result with the additional NLO contributions [6], we have subtracted from the effective squared matrix element the soft and virtual photonic contributions that have already been accounted for in σ_{s+v}. This defines

$$|\mathcal{M}^{\rm res}_{\rm eff}|^2 = |\mathcal{M}_{\rm eff}|^2 - 2f_{\rm soft,ISR}|\mathcal{M}_{\rm Born}|^2 \qquad (2)$$

which is positive even for low ΔE_γ cuts for all values of θ_γ. Convoluting this with the resummed ISR structure function for each incoming beam, we obtain a modified $2\to 2$ part of the total cross section which contains all NLO contributions and in addition includes higher order soft and collinear photonic corrections to the Born 1-loop interference. This differs from the standard treatment in the literature (*cf.* [6]) where higher order photon contributions are combined with the Born term only ("Born+").

The complete result also contains the hard non-collinear $2 \to 3$ part convoluted with the ISR structure function:

$$\sigma_{\mathrm{res},+} = \int^{\Delta(E,\theta)} dx_i \, d\Gamma_2 \, f_{\mathrm{ISR}}^{(e^+)}(x_1) f_{\mathrm{ISR}}^{(e^-)}(x_2) |\mathcal{M}_{\mathrm{eff}}^{\mathrm{res}}|^2 + \int_{\Delta(E,\theta)} dx_i \, d\Gamma_3 \, f_{\mathrm{ISR}}^{(e^+)}(x_1) f_{\mathrm{ISR}}^{(e^-)}(x_2) |\mathcal{M}^{2\to 3}|^2 \,. \tag{3}$$

The resummation approach eliminates the problem of negative weights such that unweighting of generated events and realistic simulation at NLO are now possible in all regions of phase-space.

3. NLO chargino production: results

Total cross section and relative corrections

Fig. 1 shows the c.m. energy dependence of the total LO and NLO cross section for chargino production for the mSugra point SPS1a' [1] and the relative corrections with respect to the Born result. The corrections are mostly in the percent regime and can reach 20% in the threshold region.

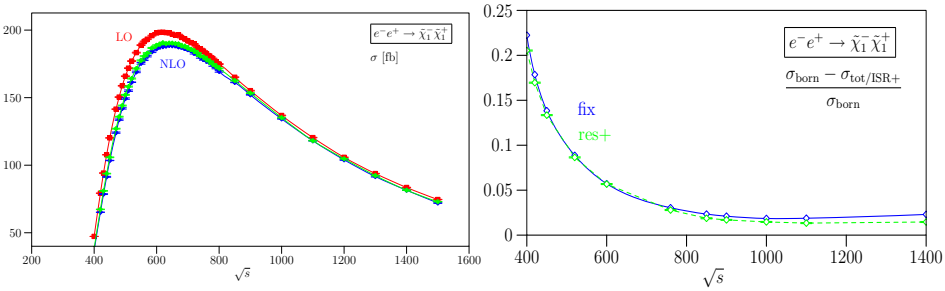

Fig. 1. Total and relative cross section as a function of $\sqrt{s}$. Left: Born (red, "LO"), fixed order (blue, "NLO") and fully resummed (green, "NLO") total cross section, right: relative fixed order (blue, solid) and fully resummed (green, dashed) higher corrections with respect to Born result.

Cutoff dependencies

Fig. 2 compares the ΔE_γ dependence of the numerical results from a semianalytic fixed-order calculation with the Monte Carlo integration in the fixed-order and in the resummation schemes. The fixed-order Monte Carlo result agrees with the semianalytic result as long as the cutoff is greater

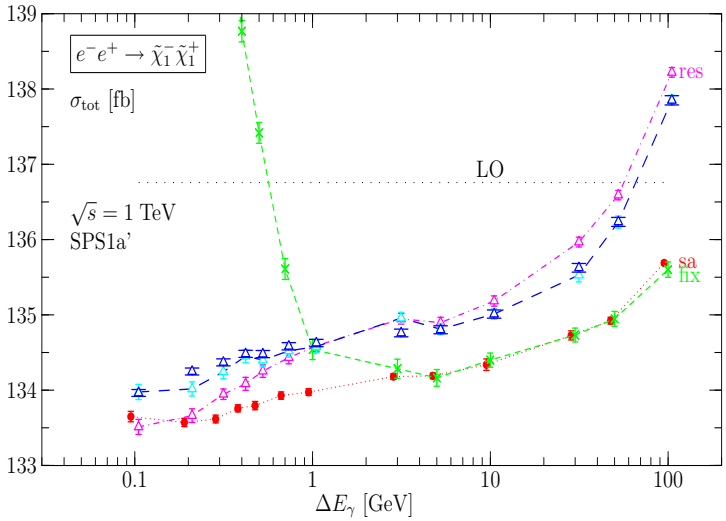

Fig. 2. Total cross section dependence on ΔE_γ: "sa" (red, dotted) = fixed-order semianalytic result; "fix" (green, dashed) = fixed-order Monte Carlo result; "res" (blue, long-dashed) = ISR-resummed Monte Carlo result; (magenta, dash-dotted) = same but resummation applied only to the $2 \to 2$ part. $\Delta\theta_\gamma = 1°$. LO: Born cross section.

than a few GeV but departs from it for smaller cutoff values because here, in some parts of phase space, $|\mathcal{M}_{\rm eff}|^2 < 0$ is set to zero. The semianalytic fixed-order result is not exactly cutoff-independent, but exhibits a slight rise of the calculated cross section with increasing cutoff due to the breakdown of the soft photon approximation. For $\Delta E_\gamma = 1$ GeV (10 GeV) the shift is about 2 ‰ (5 ‰) of the total cross section. The fully resummed result shows an increase of about 5 ‰ of the total cross section with respect to the fixed-order result which stays roughly constant until $\Delta E_\gamma > 10$ GeV. This is due to higher-order photon radiation.

For the dependence on the collinear cutoff $\Delta\theta_\gamma$, the main higher-order effect is associated with photon emission angles below 0.1°. For $\Delta\theta_\gamma > 10°$, the collinear approximation breaks down.

Event distributions

In Fig. 3 we show the binned distribution of the chargino production angle obtained using a sample of unweighted events. It demonstrates that NLO corrections to the angular distribution are statistically significant and cannot be accounted for by a constant K factor.

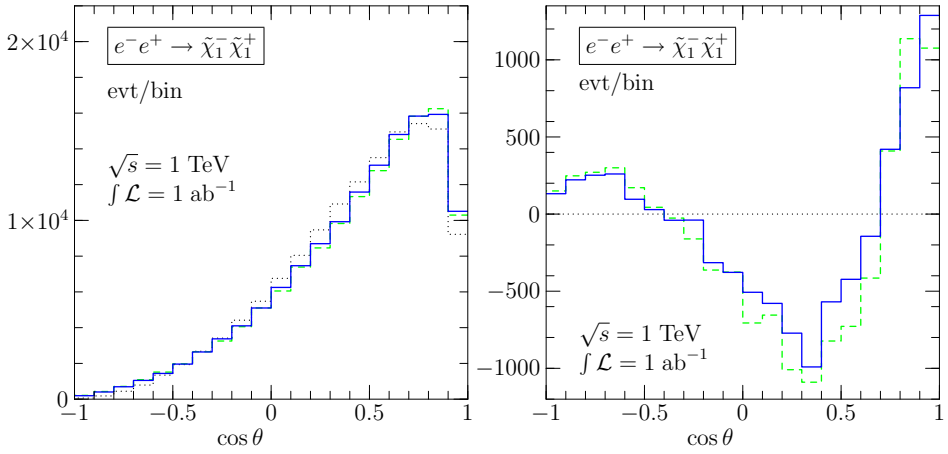

Fig. 3. Polar scattering angle distribution for an integrated luminosity of 1 ab^{-1} at $\sqrt{s} = 1$ TeV. Left: total number of events per bin; right: difference w.r.t. the Born distribution. LO (black, dotted) = Born cross section without ISR; fix (green, dashed) = fixed-order approach; res (blue, full) = resummation approach.

4. LO production and leptonic decays

Signal and (MS)SM backgrounds

In the second part of our work, we investigate the LO chargino production and subsequent leptonic decay modes. To avoid large SM backgrounds arising in the production of same flavor and opposite sign lepton pairs, we consider opposite flavor opposite sign lepton pairs in the final state:

$$e^+ e^- \longrightarrow \widetilde{\chi}_1^+ \widetilde{\chi}_1^- \longrightarrow \widetilde{\chi}_1^0 \widetilde{\chi}_1^0 e^- \mu^+ \nu_\mu \bar{\nu}_e \,. \tag{4}$$

This channel is especially interesting when the sneutrinos decay invisibly and the sneutrino pair-production channel is therefore experimentally inaccessible. In chargino pair-production and subsequent decays, however, the sneutrino and chargino masses can be determined from the edges of the lepton energy distributions [5]. The experimental signature of the signal (4) is

$$e^+ e^- \longrightarrow e^- \mu^+ + E_{\text{miss}} \,.$$

Therefore, all background processes where the missing energy results from the emission of invisible particles (ν's, $\widetilde{\chi}^0$'s) need to be considered. In addition, we have to take into account processes where additional particles are emitted at very small angles and vanish in the beam-pipe. We therefore investigate the SM and MSSM backgrounds as listed in Table I.

TABLE I

SM and MSSM background processes leading to $e^-\mu^+ + E_{\mathrm{miss}}$.

ID	Final state	Most dominant process
$\gamma\tau$	$e^+e^-e^-\mu^+\nu_\mu\,\bar{\nu}_e\nu_\tau\,\bar{\nu}_\tau$	γ-induced τ pair production (SM)
WW	$e^-\mu^+\nu_\mu\,\bar{\nu}_e$	WW production (SM)
τ	$e^-\mu^+\nu_\mu\,\bar{\nu}_e\nu_\tau\,\bar{\nu}_\tau$	τ pair production (SM)
τW	$e^-\mu^+\nu_\mu\,\bar{\nu}_e\nu_\tau\,\bar{\nu}_\tau\nu_\tau\,\bar{\nu}_\tau$	τ from WW production (SM)
γW	$e^-e^+e^-\mu^+\nu_\mu\,\bar{\nu}_e\nu_\tau\,\bar{\nu}_\tau$	γ-induced WW production (SM)
$\tilde{\tau}$	$e^-\mu^+\nu_\mu\,\bar{\nu}_e\nu_\tau\,\bar{\nu}_\tau\widetilde{\chi}_1^0\widetilde{\chi}_1^0$	$\tilde{\tau}$ pair production (MSSM)
$\tilde{\tau}\nu_\tau$	$e^-\mu^+\nu_\mu\,\bar{\nu}_e\nu_\tau\,\bar{\nu}_\tau\nu_\tau\,\bar{\nu}_\tau\widetilde{\chi}_1^0\widetilde{\chi}_1^0$	$\tilde{\tau}\nu_\tau$ from $\widetilde{\chi}$ decays (MSSM)

The values of the total cross sections for the SUSY parameter point SPS1a' including beamstrahlung and initial state radiation before the application of cuts[1] are given in Table II. The most dominant background process

TABLE II

Signal and background total cross sections before and after the application of background suppression cuts, for SPS1a' and $\sqrt{s} = 500\,\mathrm{GeV}$. ISR and beamstrahlung included. All results are given in fb, together with an integration error.

ID	Before cuts	After cuts
signal	3.940 (8)	1.905 (4)
$\gamma\tau$	25495 (4)	0.072 (1)
WW	152.42 (41)	0.794 (2)
τ	34.8 (18)	0.024 (1)
τW	2.978 (9)	0.185 (1)
γW	2.192 (12)	0.154 (1)
$\tilde{\tau}$	4.107 (7)	1.146 (2)
$\tau\,\tilde{\nu}_\tau$	2.74 (9)	0.72 (2)

is photon induced $\tau^+\tau^-$ production; its cross section exceeds the magnitude of the signal cross section by a factor 10^4. Similarly, SM background processes such as direct W and τ (pair) production are significantly larger than the signal, while SUSY backgrounds are of similar size.

[1] For numerical reasons, we always include a collinear cut of 5° for the outgoing e^-.

5. LO production and decay: Results including cuts

In order to suppress the SM and MSSM background, we apply the set of cuts given in Table III. The magnitudes for the total cross sections after the application of these cuts are presented in Table II. The signal has been

TABLE III

Cuts applied for background suppression. $\Delta\phi$ is the azimuthal separation angle of the lepton pair.

$$\begin{aligned} p_\perp(e,\mu) \geq 2\ \text{GeV}, \qquad & p_\perp(e)+p_\perp(\mu) \geq 4\,\text{GeV}, \\ 1\text{GeV} \leq E(e,\mu) \leq 40\text{GeV}, \qquad & -160^\circ \leq \Delta\phi \leq 160^\circ, \\ 15^\circ \leq \theta(e) \leq 155^\circ, \qquad & 25^\circ \leq \theta(\mu) \leq 165^\circ \end{aligned}$$

reduced by roughly a factor 2, while the dominant background from photon induced tau pair-production is now suppressed by 10^6. In total, we obtain a signal/background ratio of 0.62, which, for an integrated luminosity of $1\,\text{ab}^{-1}$, leads to a $20\,\sigma$ discovery. Fig. 4 shows the energy distribution of the leptons after cuts have been applied. While the SM processes lead to a flat background distribution which can be easily subtracted, SUSY background processes are more challenging, as they result in kinematic distributions similar to the signal.

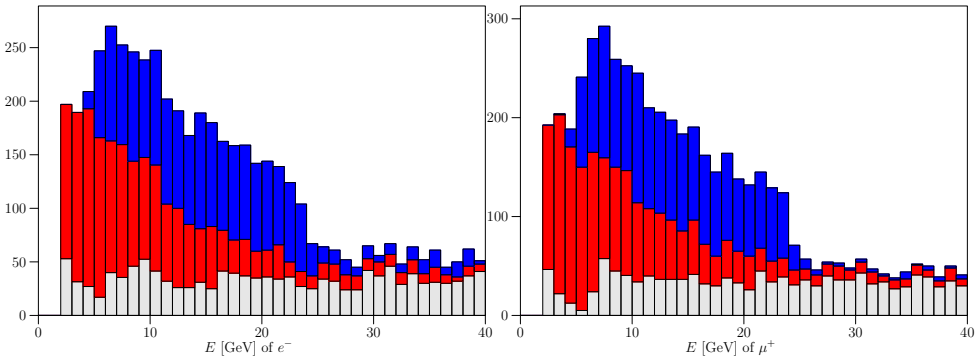

Fig. 4. Energy distribution of electron (left) and muon (right) after cuts given in Table III. Grey: SM background; (photon-induced) $\tau^+\tau^-$ and W^+W^- pair production. Red: SUSY background; $\tilde{\tau}\tilde{\tau}$ and $\tilde{\tau}\tilde{\tau}\nu_\tau\nu_\tau$ production. Blue: SUSY signal; $\widetilde{\chi}_1^+\widetilde{\chi}_1^-$ production and successive leptonic decays.

Chargino and sneutrino mass determination

In the case of quasi mass-degenerate sneutrinos and the lightest charginos, the leptonic decay mode is dominated by intermediate on-shell sneutrinos:

$$\widetilde{\chi}_1^{\pm} \to l^{\pm}\,\tilde{\nu}_l \to l^{\pm}\,\nu_l\,\widetilde{\chi}_1^0\,. \tag{5}$$

In these scenarios, sneutrino masses can only be determined from the edges in the lepton energy distributions in chargino decays (5). From on-shell relations, we obtain [5]

$$m_{\widetilde{\chi}_1^{\pm}} = \sqrt{s}\,\frac{\sqrt{E_{\min}\,E_{\max}}}{E_{\min}+E_{\max}}\,, \qquad m_{\tilde{\nu}} = m_{\widetilde{\chi}_1^{\pm}}\sqrt{1-\frac{2\,(E_{\min}+E_{\max})}{\sqrt{s}}}\,, \tag{6}$$

where $E_{\min/\max}$ are the minimum/maximum lepton energy. Taking naive read-off values for the energies, we have (*cf.* Fig. 4)

$$E_{\min} = 4.5 \pm 1.0\,\mathrm{GeV}, \qquad E_{\max} = 24.5 \pm 2.0\,\mathrm{GeV}$$

and, using (6)

$$m_{\widetilde{\chi}_1^{\pm}} = 181 \pm 15\,\mathrm{GeV}\ (183.67)\,, \qquad m_{\tilde{\nu}} = 170 \pm 14\,\mathrm{GeV}\ (173.52)\,,$$

where the values in brackets are the nominal (input) values for SPS1a'. Although the central values are in good agreement, the large errors here call for a refined treatment. Alternatively, we take the chargino mass from threshold scans; assuming $\Delta_{\mathrm{thr}}\,m_{\widetilde{\chi}} = 1\,\mathrm{GeV}$, we then obtain

$$m_{\tilde{\nu}} = 172.7 \pm 1.3\,\mathrm{GeV}\,,$$

where the error is now in the percent regime. A fitting routine for error reduction down to a permille range using edge distributions including all backgrounds is in the line of future work.

6. Conclusions

We have implemented NLO corrections into the event generator `WHIZARD` for chargino pair-production at the ILC with several approaches for the inclusion of photon radiation. A careful analysis of the dependence on the cuts $\Delta\,E_\gamma$, $\Delta\,\theta_\gamma$ reveals uncertainties related to higher-order radiation and breakdown of the soft or collinear approximations. Careful choice of the resummation method and cutoffs will be critical for a truly precise analysis of real ILC data. The version of the program resumming photons allows to get rid of negative event weights, accounts for all yet known higher-order

effects, allows for cutoffs small enough that soft- and collinear-approximation artifacts are negligible, and explicitly generates photons where they can be resolved experimentally.

Additionally, we have investigated the complete production and decay process at LO including several SM and MSSM backgrounds. For this, we used a full matrix element simulation including initial state radiation and beamstrahlung. Efficient cuts reduce the dominant background by a factor 10^6 allowing a clear isolation of the signal. The leptonic decay mode allows for mass determination of sneutrinos from the edges of the lepton energy distributions. Taking the chargino mass from threshold scans, the error of the sneutrino mass determination can be reduced to the percent level. The improvement of the mass determination precision using refined fitting routines and the combination of NLO production and decay [14, 15] are in the line of future work.

This work was supported by DFG SFB/TR9 "Computational Particle Physics", the German Helmholtz Association, grant VH-NG-005, the EU Network MRTN-CT-2006-035505 "Tools and Precision Calculations for Physics Discoveries at Colliders", and the Polish Ministry of Science and Higher Education grant No. 1 P03B 108 30.

REFERENCES

[1] J.A. Aguilar-Saavedra *et al., Eur. Phys. J.* **C46**, 43 (2006).
[2] K. Hagiwara *et al., Phys. Rev.* **D73**, 055005 (2006).
[3] W. Kilian, J. Reuter, T. Robens, *Eur. Phys. J.* **C48**, 389 (2006).
[4] T. Robens, PhD thesis, 2006, `hep-ph/0610401`.
[5] A. Freitas, W. Porod, P.M. Zerwas, *Phys. Rev.* **D72**, 115002 (2005).
[6] T. Fritzsche, W. Hollik, *Nucl. Phys. Proc. Suppl.* **135**, 102 (2004).
[7] A. Denner, *Fortschr. Phys.* **41**, 307 (1993).
[8] M. Bohm, S. Dittmaier, *Nucl. Phys.* **B409**, 3 (1993).
[9] M. Moretti, T. Ohl, J. Reuter, `hep-ph/0102195`.
[10] W. Kilian, T. Ohl, J. Reuter, `arXiv:0708.4233 [hep-ph]`.
[11] R. Kleiss *et al.,* in Proceedings *Z* physics at LEP 1, vol. 3, Geneva 1989.
[12] V.N. Gribov, L.N. Lipatov, *Sov. J. Nucl. Phys.* **15**, 675 (1972).
[13] M. Skrzypek, S. Jadach, *Z. Phys.* **C49**, 577 (1991).
[14] K. Rolbiecki, `arXiv:0710.1748 [hep-ph]`.
[15] J. Fujimoto *et al., Phys. Rev.* **D75**, 113002 (2007).